

Application of Machine Learning in Urban Base Station Placement for 5G Communications and Beyond

Irfan F. M. Rafie, Soo Yong Lim*, and Michael Jenn Hwan Chung

University of Nottingham, Malaysia

ABSTRACT: Optimal placement of wireless base stations in urban areas allows for maximum coverage and performance whilst maintaining minimal cost. In this paper, we propose a novel machine learning approach to place base stations rapidly in an urban environment for 5G communications and beyond. This is a noteworthy approach as 5G, especially those that involve millimeter wave frequencies tend to require significantly higher number of base stations for any particular area, unlike their counterpart low frequencies where a small number of base station is sufficient to cover a good geographical area. Our machine learning empowered path loss model is developed to tackle this change in gameplay head-on, and it bridges the gap between empirical and ray tracing methods where we achieve accuracy closer to ray tracing yet at a significantly lower computation cost. Promising preliminary results are obtained, with a minimum coverage area of 80% with potential for future improvements.

1. INTRODUCTION

Base station placement in urban areas has become crucial in recent times due to the use of higher frequencies in recent telecommunications technology such as Fifth Generation (5G) and beyond 5G. At higher frequencies, there is a higher amount of signal loss due to distance, penetrations, and reflection, which causes cellular coverage area per base station to decrease [1]. This in turn increases the number of base stations in an area, which demands better planning of base station placements. At high frequencies, path loss in Line-of-Sight (LoS) scenarios is more predictable than non-Line-of-Sight (NLoS) scenarios. As such, features such as building height, densities, and materials tend to influence base station coverage more [2]. An optimal base station plan should ensure acceptable Quality of Service (QoS) to user devices especially in the current era where Internet of Things (IoT) is rampant across agriculture, healthcare, and manufacturing industries. These industries rely on critical data from sensors where low QoS could cause manufacturing or medical problems. With better base station planning, the coverage in an area where base stations are already deployed could be updated with new base stations should the need arise. The world is witnessing a rapid increase of IoT and higher bandwidth requirements of mobile devices used by the general population. This is due to the requirement of catering to the increasing amount of video streams especially after the Coronavirus disease 2019 (COVID-19), which has forced businesses and education institutions to resort to teleconferencing software that can be seen by Zoom's rapid growth over 2019 to 2021 [3]. In view of this, we propose a base station placement technique that can intelligently decide the number and locations of base stations in a given urban environment. Our model is trained based on Geographic Information System

(GIS) data that was acquired from open source databases and purchased from GIS vendors. This data came in 3-dimensional space but was converted to 2.5 dimensions in order to simplify the machine learning process whilst maintaining maximum information. We previously developed a machine-learning based path loss model for propagation prediction in [4]. This path loss model is a prelude to the current paper, in that the path loss data generated from the model, along with additional data generated from other models such as empirical and ray-tracing models are now used to train the base station placement model. While the benchmark used in the previous path loss model is the standard deviation, in the current paper, we have used other benchmarks such as accuracy, coverage, and the number of base stations.

2. MODEL TRAINING

We performed our model training on an AMD Ryzen 5600 and NVIDIA RTX 3090, and it requires roughly 24 hours to train on our dataset size. We have selected a batch size of 32 as it provides the best accuracy and convergence and applies regularization and dropouts at different stages of the model. Fig. 1 shows the path loss data we plotted at 28 GHz and 60 GHz for Munich city, compared against the ray-tracing results obtained from MATLAB.

Consider that the maximum Equivalent Isotropic Radiated Power (EIRP) at 60 GHz for fixed base stations for mmWave is set to 82 dBm whereas on mobile devices, it is set to 45 dBm [5]. Our Reference-Signal-Received-Power (RSRP) values are set as follows where -105 dBm is set as our minimum acceptable received signal as shown in Table 1 according to a performance study conducted by the Federal Communications Commission (FCC) [6].

Using -105 dBm as our minimum signal strength, 82 dBm as the transmitter power, and 45 dBm for receiver power, we

* Corresponding author: Soo Yong Lim (Grace.Lim@nottingham.edu.my).

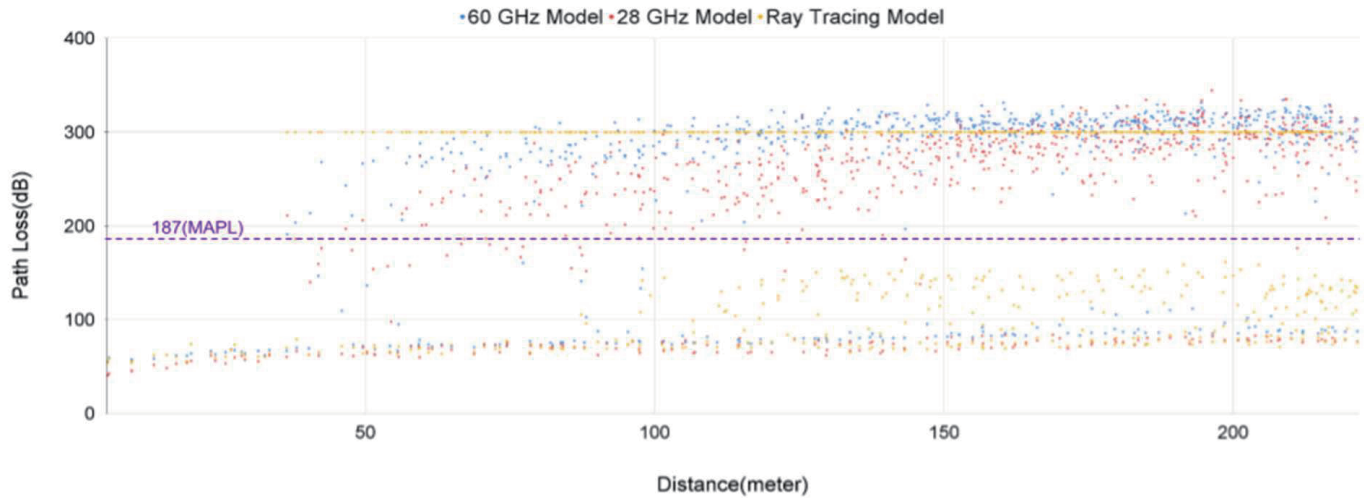


FIGURE 1. Path loss data at 28 GHz and 60 GHz for Munich City.

TABLE 1. RSRP Table.

Signal Strength	RSRP(dBm)	Description
Excellent	−80 to −60	Strong signal, Ideal for High-Speed Data
Good	−90 to −80	Reliable signal, Ideal for Normal Speed Data
Fair	−105 to −90	Weaker signal, degraded performance in data transfer
Poor	−105 and below	Very weak signal, with potentially frequent disconnects with slow speed

can calculate our Maximum Allowable Path Loss (MAPL) as shown below [7]:

$$MAPL = power_{tx} - minimumsignalstrength - power_{rx}$$

which results in an MAPL of **187 dB**.

Path loss values below the MAPL of 187 dB are considered reachable by our transmitter, and values above that are considered unreachable and not measurable in real life due to signal loss. This allows our model to discern locations which are reachable and unreachable for base station placement. In Fig. 1, the LoS points are accurately predicted, and our model can also predict accurate values in nLoS areas where diffraction occurs. However, our model still attempts to predict values in nLoS areas that are unreachable resulting in path loss values above 187 dB as our path loss prediction is performed without the model knowing which locations are reachable and unreachable. This allows our model to determine locations which are unreachable and which are reachable.

As the path loss prediction values go above 187 dB, the signal is unreachable in both ray tracing and in measurements using standardized equipment on both transmitter and receivers across the entire scenario.

The Root Mean Squared Error (RMSE) value comparison between our 28 and 60 GHz models is 5.96 dB for LoS scenario, and 18.09 dB for NLoS scenario after removing sparse data locations which are unreachable via raytracing simulation. This removal of data is justified as these locations are unreachable in our training data, yet our model is attempting to predict locations which are unreachable and unmeasurable in raytracing

simulations and in real life. This LoS value is close to the calculated free space path loss (FSPL) values, which is 6.61 dB, but we note that for the NLoS scenario, the recorded RMSE value is less desirable.

3. BASE STATION PLACEMENT MODEL

In this section, we present our machine-learning empowered base station placement model.

3.1. Factors Affecting Placement

There are several major factors that affect base station placement, namely, coverage, cost, quality, and capacity [8]. The quality factor is defined by the signal-to-interference-plus-noise ratio (SINR). As the path loss value increases, the SINR value at the receiver location will be significantly affected leading to a reduced level of connection quality [9]. In our tests, LoS is a major factor that is highly weighted. Taking 60 GHz for instance, the base stations are essentially LoS locked in order to maintain connectivity in cases of bad weather as frequencies above 10 GHz is affected by water vapor and oxygen particles [10–12].

3.2. Location Preparation

In order to generate a map of optimized base stations, we first have to prepare the map for locations where it is possible to place base station. This can be adjusted depending on the preference of the supplier and radio equipment as different frequen-

cies have different expectations in base station height where 5G picocells operate at a height of 5 to 10 meters whereas 3G base stations require a taller transmission tower. The accuracy level should also be set at this stage. For example, an accuracy of 1 meter should have receivers 1 meter away from each other, providing us with 1 meter grid. The accuracy level can be set to be higher or lower depending on the requirements. In our tests, this accuracy level is set to 3 meters. We decided on 3 meters in order to accelerate the tests whilst still having high enough accuracy that we can simulate path loss along roadways and pathways capable of pedestrian traffic. This generation procedure draws us a grid map of valid transmitters and receivers locations in an area. This generated grid map is then used to create our paired image dataset. This grid map allows us to place transmitters and receivers rapidly as we can look up grid coordinates that are relevant to a transmitter location. This improves our base station optimization system as all the image information has already been prepared prior to optimization. With every different frequency band, we set an expected hard limit distance in order to improve the optimization time. This limit is set if the FSPL value increases over the acceptable limit where the SINR does not allow for reliable communication between the transmitters and receivers. This is checked using the transmitter and receiver parameters that are described next in the model description.

3.3. Model Description

Previous literature shows that base station planning models can be performed heuristically or via integer linear programming (ILP) [13, 14] using techniques described below:

1. Greedy Addition
2. Binary Integer Linear Programming (BILP)
3. Convex Linear Programming

Our model is a mix of Greedy Addition and Binary Integer Linear Programming where we have set receiver grids across the entire scenario map, and they are marked as being covered by base stations or not. These grids are updated additively iteration by iteration after our model predicts the best possible location to place the next base station given the location of already placed base stations as well as currently covered receiver locations.

However, previous literature mostly only includes base station placement with only using formula-derived path loss models which rely mainly on distance as a parameter. Whilst distance is one of the parameters that hold the most weight in calculating path loss, other factors in these models are simplified into constants, resulting in higher RMSE values in path loss calculation than ray-tracing and being able to take into account different transmission properties in an urban environment. Although at 28 GHz and 60 GHz, mainly nLoS path loss values are used as shown in [15], there are non-negligible transmission path loss values in nLoS areas which are not utilized by previous literature.

Our proposed model has the potential to optimize base stations using a more versatile path loss prediction method that takes into account more site-specific information such as fo-

liage, minor obstructions, and major obstructions and accounts for more than only distance-based LoS path loss values.

3.4. Model Process

The model that we use for base station optimization has a relatively simple goal, which is to minimize the amount of blank space in a scenario map grid of receiver locations while maintaining a minimal number of transmitters. The model will prioritize placing transmitters that can provide the most coverage adjacent to previous transmitters while maintaining a minimal overlap. The initial placement of the first base station in our scenarios can be determined by the model or set by the user to overlap currently existing infrastructure. Both methods have their advantages and disadvantages where a randomly placed primary base station might have a better optimization result than the manually placed version. However, using a manually placed base station offers other advantages. After the placement of the first base station, our optimization process begins by adding a second transmitter location and predicts the path loss values for the area around it. This process repeats itself by adding more transmitters until the desired coverage is achieved. The placement of the subsequent transmitter locations is determined by our model, and the coverage level is checked on every transmitter addition. A dataset of current coverage is updated for every transmitter addition. This allows us to determine coverage overlaps and determine whether to update the newly added transmitter location or to remove the previous transmitters. Over time, the model will maximize coverage within the specified scenario area. As it is impractical for the model to end on a single solution, we will accept any base station placement solutions that fulfill the set target coverage criteria. Every receiver grid coordinate from our grid map dataset is marked in our database, it either is empty indicating no coverage yet or includes path loss values from the various transmitter locations if it is covered. As an example, a receiver location at a particular coordinate x and y has 3 valid path loss values, 119 dB, 99 dB, and 95 dB, with each of them being linked to transmitters 1, 4, and 6, respectively. This indicates that transmitters that were generated during the 6th epoch are capable of providing maximum performance to this location. Then, transmitter 6's coverage is analyzed where the coverages prior and post addition are compared. Our performance metric for base station optimization is such where we calculate the coverage score out of the whole scenario map starting at 0% coverage consisting of total possible receiver units in the area spaced regularly, which is 3 meter grids in our test at 1.6 meters of height. If a receiver location is covered by any transmitter, the coverage score increases by 1 unit. If a receiver location receives an improvement by a new transmitter, the score is compared to determine whether the new addition is an upgrade or a waste of resources. As an example scenario, if a single transmitter is capable of reaching 200 receiver locations, and the whole map consists of 15000 receiver locations, we update our global coverage score as 1.3% covered after the first epoch relative to 0% covered prior. Every single receiver location that has never been covered before, and covered by a new transmitter increases our coverage score by 1 unit; however on any following epochs,

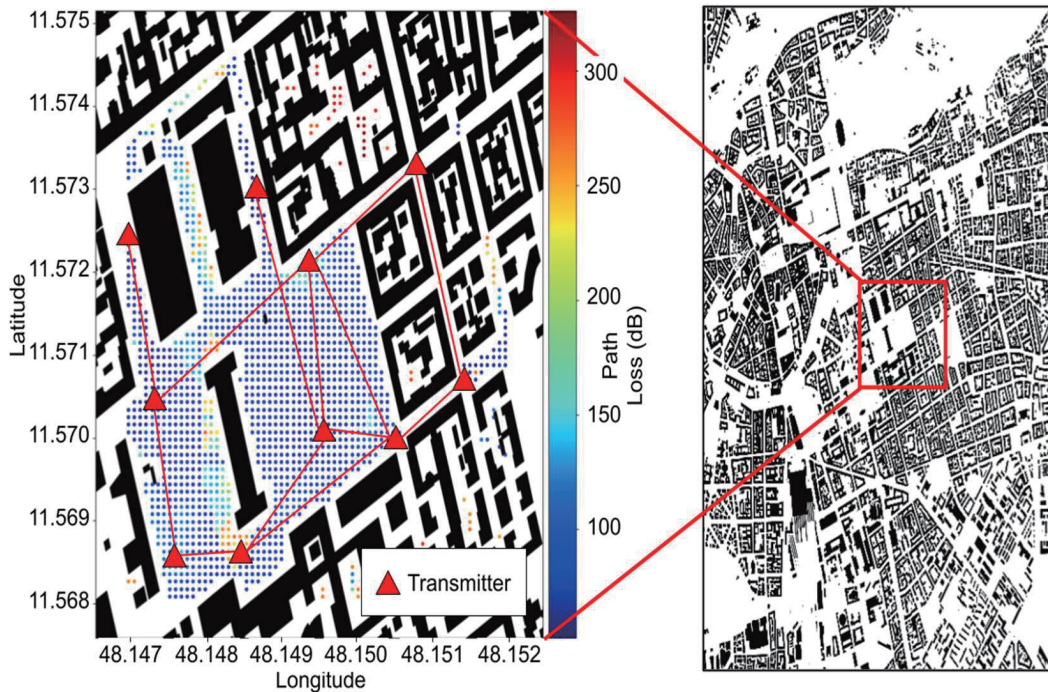


FIGURE 2. Base station optimizer crop.

an improvement to an already covered unit only increases our score by partial amounts. This allows us to determine whether a new transmitter overlaps a previous transmitter minimally or is majorly overlapping causing wasted resources. If the coverage score does not improve significantly enough, the latest transmitter addition is removed, and a new transmitter is placed in a different location, and the coverage score is rerun again. This process is looped continuously until our required specifications are achieved, which is set to be a minimum of 80% coverage with minimal overlap between transmitters and minimal base station count. Our generative model is an optimization model where we use the current coverage map as our score metric. For example, in Fig. 2, our entire scenario map encompasses a total of 1132560 coordinate points which are equal to a coordinate point every 3 meters on the x and y axes.

In Fig. 2, an illustration of the base station optimizer crop is shown. The gap between these coordinate points can be adjusted depending on the accuracy of which the optimizer will run at the cost of increased computation time when the gaps are decreased. In order for a transmitter to be placed, it has to fulfill several conditions especially at mmWave frequencies. First of all, these nodes have to be in a range of another transmitter under the assumption that it will perform backhaul services for the network whilst servicing user devices. If the proposed node has more than 1 link to a different transmitter, the node is scored higher in our model as it allows for more redundancy if a single backhaul link fails. This interconnectivity is shown in Fig. 2 via the red lines connecting between transmitters.

In Fig. 3, the placement method per iteration is shown. The distance between transmitters has to be outside of a certain distance in order to prevent overcrowding of transmitters in a single point. To determine the potential base stations locations,

several steps are performed, where transmitter A is the first base station placed, and transmitters B and C indicate 2 other possible positions for transmitters. In Fig. 3, transmitter C is selected as the next base station to be placed since it achieves a better score than transmitters D or B. Our placement method is described as follows:

1. The base station dataset begins with 0 base stations and is only provided by the scenario map. The current coverage score in this scenario is **0%**.
2. Transmitter A is placed by the model randomly, or its position can be specified to currently deployed base stations for 3G/4G as existing infrastructure. When being placed randomly by the model, it will prefer areas which have a higher probability of LoS paths to surrounding areas. In this example scenario, transmitter A has improved the coverage score by 30%, resulting in a scenario score of 30% coverage.
3. The second base station can only be placed within the shaded area of the ring surrounding transmitter A. A minimum distance limit is set in order to prevent overcrowding of transmitters during placement thus reducing the amount of iterations of correcting these overlapping locations. The maximum distance limit is set based on the distance where transmission at the set frequency is no longer feasible due to attenuation in free space without accounting for path loss due to obstruction and diffraction. This is set in order to reduce the number of base stations that qualify to be placed as the link to transmitter A. Our possible transmitter locations are B, C, D, and E.
4. In consideration that we are optimizing for mmWave picocells with expectations of them performing backhaul,

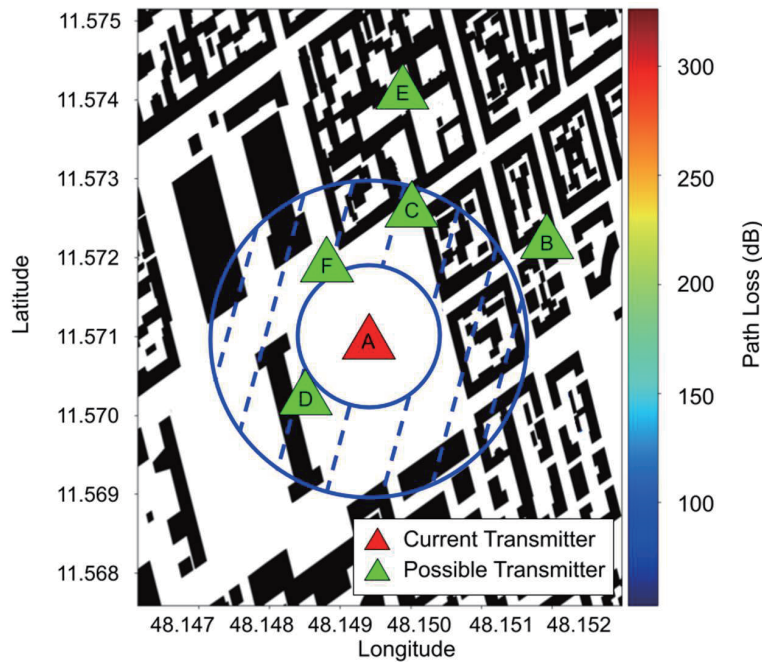


FIGURE 3. Placement method per iteration.

LoS is required between base stations, disqualifying transmitters B, E. In cases where backhaul is not performed, this limitation can be removed, allowing for optimization for maximum coverage without regard to LoS in between base stations. Frequencies that are LoS-dependent such as mmWave have a significantly higher weight to LoS availability leading to each transmitter requiring a LoS of at least one other base station.

- Our machine learning based path loss prediction model predicts the path loss values and coverage for transmitter locations C and D where if transmitter D is placed, an improvement of 3% is observed whereas if transmitter C is placed, an improvement of 6% is observed. Thus, transmitter C is placed, and the current scenario map is updated to have transmitters in locations A and C with a coverage score of 36%. In every base station addition, a comparison in path loss values in the already covered areas is performed in order to determine if a more recently placed base station can have better coverage than previously optimized areas. An example would be the placement of transmitter F, which not only covers the area that transmitter C covered, but also improves the overall coverage score by an extra 2%, yielding a total coverage score of 38% instead of 36%. Transmitter C will be removed and replaced with transmitter F. This results in a constantly optimizing model removing current base stations if they are redundant and have worse path loss quality in the area.
- Steps 2 to 5 are repeated using the current transmitters list which contains Transmitters A and C. New possible transmitter locations are spawned surrounding the current transmitters list and used in Steps 2 to 5. During this process, the overall base station coverage score is updated according to the current transmitters list until the required

coverage score is reached. This results in a base station map where the number of base stations is computed and optimized with every iteration.

4. RESULTS AND DISCUSSION

As can be seen in the left-hand side of Fig. 2, a scenario map with the rough size of 0.42 km² only uses 8 base stations at the frequency of 60 GHz in order to reach the minimum acceptable coverage of 80%. Within this scenario, our model's base station counts for 28 GHz and 60 GHz are similar due to similar transmission properties that are heavily dependent on LoS.

Our coverage score in our entire scenario yielded a coverage of 74.08% of the entire map where the MAPL for receivers is defined as 187 dB and an MAPL of 130 dB for base station to base station links. This, however, includes areas which are unreachable because they are enclosed by walls higher than the specified transmitter height such as transmitter E as shown in Fig. 3. These areas cannot be reached by LoS and nLoS signals from any transmitters surrounding the area without adding extra parameters such as antennas or base stations above the building height. Thus, we remove these areas from our calculations as they are deemed impossible to reach, resulting in a coverage score of 85.4% across the entire scenario map, which is remarkable. Furthermore, the model will continue to attempt optimizing the base station locations until the minimum coverage target is reached which has been defined as 70%. A higher coverage target such as 80% and 90% will incur costs such as longer computation time and increased base station count.

Our results corresponding to coverage score and base station count are as in Table 2 where the maximum receiver node count is 1524 for the entire scenario.

TABLE 2. Base station improvement per iteration.

Base Station Index	Tx-specific Average Path Loss (dB)	Rx Nodes Covered (≤ 187 dB)	Newly Covered Nodes	Overall Nodes Covered	Initial Coverage Score (%)	Actual Coverage Score (%)
0	83.50	515	515	515	33.79%	38.96%
1	97.85	313	88	603	39.57%	45.63%
2	88.52	423	59	662	43.44%	50.09%
3	70.67	367	88	750	49.21%	56.75%
4	77.97	213	104	854	56.04%	64.63%
5	85.46	429	24	878	57.61%	66.44%
6	102.69	663	51	929	60.96%	70.30%
7	75.52	443	75	1004	65.88%	75.97%
8	79.14	300	101	1105	72.51%	83.62%
9	89.37	16	16	1121	73.56%	84.83%
10	86.93	8	8	1129	74.08%	85.43%

In Table 2, we show the improvements after each base station addition. Our model begins with 0 base stations, and Base Station with Index 0 is added. Base Station 0 has 515 receiver locations that have path loss values below the MAPL of 187 dB. This improves our coverage score from 0.00% to 33.79%. Every base station addition will only occur if it improves the coverage % or if it improves the quality of coverage in the area, depicted by their average path loss value if the number of newly covered areas is low compared to the minimum improvement count set by the user. In this scenario, we are only looking for the minimum number of base stations to cover 70% of the scenario, and the optimization can stop at Base Station 8. If only 60% coverage is required, the optimization process will stop after placing Base Station 6. As we can see, as the required coverage % increases, fewer new nodes are covered as shown in Base Stations 9 and 10. We can also note that after each Base Station addition, it does not increase the overall covered nodes similar to the number of receiver locations that the base station covers. This is due to the base stations improving the path loss of previously covered receiver nodes. An example is Base Station 1 covering 313 nodes out of 1524 in the scenario map, but only 88 are new nodes, and 225 are improvement to already current nodes. This optimization will continuously occur, and if an early base station is considered redundant, and new base stations can have better coverage and better path loss average, it will replace the old base station.

Furthermore, the overall coverage score also includes areas which are unreachable as explained in Section 2. In this scenario, 203 receiver nodes are not reachable at 28 GHz and 60 GHz due to the areas being surrounded by buildings such as courtyards similar to the location of transmitter F in Fig. 3. Thus, we can remove 203 nodes from our maximum node count, resulting in our actual coverage scores where 8 base stations fulfill our 80% coverage requirement. The optimization model can run perpetually, whilst trying to improve the base station count; however, improvements to coverage score will be increasingly marginal as the number of base stations increases.

In comparison to the results of Binary Integer Linear Programming in a previous literature where 16 base stations are deployed in an area of 1 km² [13] with a coverage score of 90%, our model places 8 base stations in an area of 0.42 km² with a coverage score of 85.4%. As different cities have different architectural designs, path loss propagation in the area may vary resulting in slightly differing base station numbers. This shows that our model is comparable to previously used models [13, 16]. However, our model has a more dynamic path loss prediction method not limited to LoS situations with an increased accuracy to nLoS situations alongside the capabilities for base stations to be placed at any locations not limited to building walls which allows for greater versatility in potential base station locations.

In addition, we recorded a speed of 4 ms per path loss calculation assuming a similar performance computer specified in [4]. Our model when being performed using machine learning path loss models has theoretically fastest speed of 90 seconds if we assume no overhead on processing. Comparing this to ray-tracing model, it would take significantly longer at 76 minutes if the timing is scaled linearly. However, ray-tracing path loss model does not scale linearly and only increases in difficulty as the distance between transmitter and receiver increases in nLoS scenarios. Thus, we can expect a significantly longer time to reach this level of optimization if a ray-tracing path loss model is used.

5. CONCLUSION

In conclusion, machine learning can significantly improve the speed of optimization process of base station placement when it is paired with a machine learning-based path loss model system. When being paired with our path loss model, a single transmitter-receiver pair's path loss value can be predicted in 4 m/s. Empirical methods can perform this in the scale of nanoseconds but not at the same level of accuracy. Ray-tracing, on the other hand, requires a longer time that a full city prediction becomes unfeasible without the help of powerful com-

puter machines. The biggest advantage of our placement system is that the prediction times are static and do not scale. For extremely simple cases, this method might have a longer runtime than any other method due to preprocessing overheads; however, as the size of prediction area increases, our method will have a lower prediction time. For future work, further improvement to the placement and minimization of base station count can be done by tuning the optimization model and possible placement positions such as dynamic antenna height parameters where the antenna height can be optimally determined by the model in order to circumvent issues such as unreachable areas described in Section 4 and Fig. 3.

REFERENCES

- [1] Sun, S., G. R. MacCartney, and T. S. Rappaport, "Millimeter-wave distance-dependent large-scale propagation measurements and path loss models for outdoor and indoor 5G systems," in *2016 10th European Conference on Antennas and Propagation (EuCAP)*, 1–5, Davos, Switzerland, Apr. 2016.
- [2] Friis, H. T., "A note on a simple transmission formula," *Proceedings of the IRE*, Vol. 34, No. 5, 254–256, 1946.
- [3] Zoom, "Zoom video communications Q1 FY22 earnings," [Online]. Available: <https://investors.zoom.us/static-files/2d917a17-6ad3-49f7-9642-2fb138f5ff84>, 2021.
- [4] Rafie, I. F. M., S. Y. Lim, and M. J. H. Chung, "Path loss prediction in urban areas: A machine learning approach," *IEEE Antennas and Wireless Propagation Letters*, Vol. 22, No. 4, 809–813, 2023.
- [5] Federal Communications Commission, "Revision of Part 15 of the commission's rules regarding operation in the 57–64 GHz band," [Online] Available: <https://docs.fcc.gov/public/attachments/FCC-13-112A1.pdf>, Oct. 2024.
- [6] Federal Communications Commission, "Mobility fund phase II coverage maps investigation staff report," [Online] Available: <https://docs.fcc.gov/public/attachments/doc-361165a1.pdf>, Oct. 2024.
- [7] Tolstrup, M., *The Link Budget*, 361–388, Wiley, 2015.
- [8] Amine, O. M. and A. Khireddine, "Base station placement optimisation using genetic algorithms approach," *International Journal of Computer Aided Engineering and Technology*, Vol. 11, No. 6, 635–652, 2019.
- [9] Haenggi, M., J. Andrews, F. Baccelli, O. Dousse, M. Franceschetti, and D. Towsley, "Guest editorial: Geometry and random graphs for the analysis and design of wireless networks," *IEEE Journal on Selected Areas in Communications*, Vol. 27, No. 7, 1025–1028, 2009.
- [10] Shayea, I., T. A. Rahman, M. H. Azmi, and M. R. Islam, "Real measurement study for rain rate and rain attenuation conducted over 26 GHz microwave 5G link system in Malaysia," *IEEE Access*, Vol. 6, 19 044–19 064, 2018.
- [11] Bureau, I. R., "Recommendation ITU-R p.530-18 propagation data and prediction methods required for the design of terrestrial line-of-sight systems p series radiowave propagation," [Online]. Available: <http://www.itu.int/ITU-R/go/patents/en>, 2022.
- [12] Zhu, Y., Z. Zhang, Z. Marzi, C. Nelson, U. Madhow, B. Y. Zhao, and H. Zheng, "Demystifying 60 GHz outdoor picocells," in *Proceedings of the 20th annual international conference on Mobile computing and networking*, 5–16, 2014.
- [13] Palizban, N., S. Szyszkowicz, and H. Yanikomeroglu, "Automation of millimeter wave network planning for outdoor coverage in dense urban areas using wall-mounted base stations," *IEEE Wireless Communications Letters*, Vol. 6, No. 2, 206–209, Apr. 2017.
- [14] Anjinappa, C. K., F. Erden, and I. Güvenç, "Base station and passive reflectors placement for urban mmWave networks," *IEEE Transactions on Vehicular Technology*, Vol. 70, No. 4, 3525–3539, Apr. 2021.
- [15] Jacob, M., S. Priebe, R. Dickhoff, T. Kleine-Ostmann, T. Schrader, and T. Kurner, "Diffraction in mm and sub-mm wave indoor propagation channels," *IEEE Transactions on Microwave Theory and Techniques*, Vol. 60, No. 3, 833–844, Mar. 2012.
- [16] Szyszkowicz, S. S., A. Lou, and H. Yanikomeroglu, "Automated placement of individual millimeter-wave wall-mounted base stations for line-of-sight coverage of outdoor urban areas," *IEEE Wireless Communications Letters*, Vol. 5, No. 3, 316–319, Jun. 2016.